Nuclear hormone receptor regulation of Caudal mediates ventral nerve cord assembly in *C. elegans*.

Nathaniel Noblett,[1,2] Tony Roenspies,[1] Stephane Flibotte,[3] and Antonio Colavita[1,2]

[1]Neuroscience Program, Ottawa Hospital Research Institute, Ottawa, Canada
[2]Department of Cellular and Molecular Medicine, University of Ottawa, Ottawa, Canada
[3]UBC/LSI Bioinformatics Facility, University of British Columbia, Vancouver, Canada

Highlights

- *pal-1* mutants display neuron positioning defects in the ventral nerve cord (VNC).
- The embryonic expression of *pal-1* in DD and DA neurons is regulated by an upstream promoter element.
- PAL-1 is involved in rosette-mediated convergent extension during VNC formation.
- The nuclear hormone receptor SEX-1 is for required for proper VNC assembly.
- Knockdown of *sex-1* causes loss of PAL-1 expression in VNC neurons.

Abstract

The regulatory network governed by CDX transcription factors in mammals and their ortholog PAL-1, in *C. elegans*, play critical roles in early nervous system development. In nematodes, proper expression of PAL-1 is required for assembly and extension of the ventral nerve cord (VNC). Despite this importance, how PAL-1 is regulated in the nervous system and its precise role remains unclear. We identified an upstream regulatory region within the *pal-1* promoter that drives *pal-1* expression in a subset of DD and DA neural progenitors during VNC assembly. We have identified a Loss of *pal-1* in motor neuron progenitors leads to delays in multicellular rosette formation and resolution during VNC formation. We show that a region upstream of the promoter as well as in the nuclear hormone receptor sex-1 result in complete loss of PAL-1 expression in two subtypes of VNC neurons. Restoration of PAL-1 in the VNC through extrachromosomal expression is sufficient to rescue assembly defects in *pal-1* and partially rescue defects in *sex-1* mutants. Together, our findings suggest that tissue-specific activity facilitates convergence-extension in the *C. elegans* VNC during its' assembly. Given the role of CDX and planar cell polarity proteins during neural tube formation in mammals, this work may provide insights and further tools to examine regulatory pathways during nervous system development.

Keywords

C. elegans, Morphogenesis, Convergent extension, Ventral nerve cord, *Caudal*, PAL-1, SEX-1

Introduction

The coordination of signaling cascades and positional information through transcriptional networks is essential for axial extension during embryonic morphogenesis. The caudal family of homeodomain transcription factors, including CDX1/2/4 in mammals and their worm ortholog PAL-1, play critical roles in axial extension by coordinating pathways involved in cell-fate determination, morphogenesis and regionalization (Waring and Kenyon, 1991; Edgar et al., 2001; Zhu and Lohnes, 2022). For CDX proteins this includes the regulation of neurulation

during mammalian development, a process where the neuroectoderm folds and elongates to form the neural tube (Savory et al., 2011; Zhao et al., 2014). Neurulation is partly driven by rosette-mediated convergent extension, a process characterized by coordinated cell-cell intercalations along the mediolateral axis and extension along the anterior-posterior axis. Mouse embryos with mutations in both CDX1 and CDX2 exhibit typical convergent extension defects, including a reduced length-to-width ratio of the neural tube, failure of extension, and a broadened midline of the neural plate. As a result, these defects lead to embryonic lethality and craniorachischisis, a severe neural tube defect.

CDX proteins function as a central hub for multiple signaling pathways that regulate neurulation (Wilson et al., 2003; Palmer et al., 2021; Zhao et al., 2022). This includes direct induction of CDX1 by retinoic acid receptors α1 and γ (RARs), ligand dependent nuclear hormone receptors, and β-catenin, a key component of canonical WNT signaling (Houle et al., 2003; Zhao et al., 2014). Signalling through CDX members during neurulation is at least partially mediated by the regulation of the Planar Cell Polarity (PCP) pathway (Savory et al., 2011). This includes the key components Scribble and transmembrane receptor PTK7 (Wehner et al., 2011; Hayes et al., 2013; Martinez et al., 2015). Knockout of both CDX1 and CDX2 interacts genetically with the Scribble. Both CHiP analysis and transfection assays also suggest that CDX proteins regulate PTK7 expression. While the direct implication of CDX transcription during neurulation are poorly understood, the family has been shown to regulate cytoskeletal movements and remodeling in the intestinal epithelium of colon cancer cells (Lorentz et al., 1997; Keller et al., 2004). Across multiple cell types, changes to CDX1 and CDX2 expression levels is sufficient to alter adhesive properties and cytoskeletal associated protein function. This aligns with the role of PCP activity during neurulation, which polarizes cytoskeletal activity (Ybot-Gonzalez et al., 2007; Shindo et al., 2019; Devitt et al., 2024).

Compared to mammalian neurulation, less is understood about how PAL-1 may link signalling mechanisms during the regulation of cell fate determination, regional identity, and morphogenesis. Expression of the gene is required in P2 blastomere descendants, including a dominant role in establishing the fate of C/D cell lineages (producing primarily body-wall muscle, hypodermal cells, along with two neurons) and a synergistic role in establishing E cell lineages (producing intestinal cells) along with WNT effector POP-1 and bZIP transcription factor SKN-1 (Hunter and Kenyon, 1996; Maduro et al., 2005). As part of its role, PAL-1 transcription regulates the expression of transcription factor cascades which establish the identity of C cell descendants (Baugh et al., 2005). These include factors belonging to the homeodomain, zinc-finger, GATA, MADS domain and bHLH families which span epidermal, muscle, and posterior lineages (Baugh et al., 2005). Additional work has shown that loss of *pal-1* disrupts non-cell fate related functions, suggesting that some of its roles in morphogenesis may be conserved (Gilbert et al., 2020). This includes orienting epidermal seam-cell migration and alignment during development. Other defects, including delays in ventral enclosure, failed long range migration in MS cell descendants and abnormal cleavage axis in muscle cells suggest that additional functions of a *pal-1* network remain to be explored (Edgar et al., 2001).

Ventral nerve cord (VNC) formation in *C. elegans* shares several core features with neurulation in mammals, including rosette mediated-convergent extension and asymmetric distribution of core PCP components (Shah et al., 2017). At hatching, the VNC is comprised of 22 embryonically born neurons, belonging to three sub-types (DA, DB, DD), which together with their axons form a tract that runs along the anterior-posterior axis of the worm. Neurons are

born during mid-embryogenesis from lineages originating on the left and right of the embryo. Coincident with the narrowing of the ventral epidermis, VNC neurons move towards the embryonic midline and undergo a series of intercalations. This includes the assembly of multicellular rosettes. These embryonic movements position the neurons along a single file in a stereotypical order as the worm elongates prior to hatching. VNC assembly depends on multiple signals to are required for convergent extension, including conserved PCP members, inositol phosphate biosynthesis and SAX-3/ROBO (Shah et al., 2017; Noblett et al., 2024). When these factors are lost, multicellular rosettes dynamics are disrupted, proper cell intercalation fails and the resulting neurons of the VNC are mispositioned and disordered.

Here, we describe how *C. elegans* PAL-1 functions during VNC formation. Using an allele which produces tissue-specific changes in gene expression, we have identified that the role of *pal-1* extends to controlling movements of neuronal progenitors during VNC formation. We found failures in intercalation between neurons and delays in the resolution of a central rosette, features characteristic of defective convergent extension. These defects subsequently lead to mis-ordering of motor neuron subtypes and a significant shortening of the VNC in post-hatching worms. Additionally, we show that tissue-specific expression of *pal-1* is regulated by an upstream enhancer region and requires the nuclear hormone receptor SEX-1. Loss of *sex-1* phenocopies both the larval defects and the expression changes caused by loss of the upstream enhancer. These findings reveal a novel regulatory pathway in nematode nervous system development and highlight conserved mechanisms in central cord formation.

Results

Identification of a genomic region associated with tissue specific regulation of pal-1.

We have previously reported conducting a screen using the DD-specific reporter flp-13p::GFP in order to identify genes that disrupt embryonic VNC morphogenesis (Noblett et al., 2025). Whole genome sequencing of two mutants isolated from this screen identified *zy43* and *zy44* as SNPs in a non-coding region upstream of the caudal ortholog *pal-1* and *arl-6* (Fig1B). While this upstream region lay near the loci for *arl-6*, mutation in the gene did not recapitulate the phenotypes found in either allele (data not shown), we therefore examined *pal-1*. To facilitate further investigation of a possible role for PAL-1, we knocked-in an endogenous GFP reporter to the native pal-1 loci using CRISPR/CAS9. PAL-1 is expressed in a variety of cells within the tail, which have been previously shown (Fig1C) (Edgar et al., 2001). In addition, the protein is expressed within a subset of cell of the VNC, including mid- to posterior DB and DD neurons (approximately DB4-7, DD4-6) and mid DA neurons (approximately DA4-6).

Previous data regarding CDX family members has suggested similar regulation by regions upstream of the transcriptional start site is required for tissue specific expression (Wang and Shashikant, 2007). Additionally, work involving *pal-1* has shown that a large region upstream of the promoter is needed in extrachromosomal transgenes to facilitate complete rescue of defects (Edgar et al., 2001). To further investigate this region, we used Cas9 to generate a deletion which overlapped both single base pair changes (*zy117*). Making use of the existing endogenous GFP reporter, we repeated the fluorophore knock-in to examine the effect of the deletion on WT *pal-1* expression (Fig1D). Strikingly, in contrast to expression of PAL-1 in the tail, mutants almost completely lack expression in the DD and DA neurons. The exception

appears to be DB neurons, which can be easily identified prior to intercalation at the midline. These appear to retain their expression.

Pal-1 mutants display larval phenotypes associated with CE defects.

Mis-regulation of convergent extension during VNC assembly has been shown to facilitate positioning defects amongst motor neuron subtypes (Shah et al., 2017; Noblett et al., 2024). To determine the extent to which PAL-1 participates in VNC assembly, we measured several CE related defects in *zy117*. *pal-1* mutant larvae display a strong anterior shift amongst DD neurons and minor shifts amongst DA and DB neurons (Fig2A and B). Defects in pal-1 mutants are predominantly amongst neurons which express PAL-1, with some minor defects in DD1 and DD2. We also noted that the stereotypical order of VNC motor neuron subtypes was perturbed (Fig2D). The three neuron subtypes typically form a repeating pattern that persists across the VNC, consistent with the arrangement of motor units. Loss of *pal-1* leads to significant changes in the order of most mid-posterior VNC neurons. Consistent with a role in facilitating intercalations, we also noted that a small proportion of neurons failed to arrange into a single file by the time of hatching. These sets of neurons (most often containing DBs) end up oriented along the dorsoventral axis.

Several studies have commented on the role of PAL-1 in regulating cell lineages, with its loss particularly affecting blastomere lineages which produce hypodermal, muscle and intestinal cells (Edgar et al., 2001; Maduro et al., 2005). As OU792 contains three reporters which are driven by genes involved in terminal motor neuron fates, we were able to assess if defects resulting from pal-1 loss were a result of altered morphogenesis or cell-fate. The consistency of expected and observed numbers of in DA, DB and DD neurons suggested that the defects in *zy117* were not a result of terminal cell-fate changes.

PAL-1 fails to genetically interact with either the canonical or non-canonical WNT pathways.

In mammals, CDX family members contribute to neurulation and convergent extension through regulation of the PCP pathway (Savory et al., 2011; Zhao et al., 2014). Similarly, the simultaneous deletion of both *vang-1* and *sax-3* leads to an increase in the anterior displacement of VNC neurons, a result that suggests severe disruption in CE movements (Shah et al., 2017). Given that loss of core PCP protein like VANG-1 result in anterior shift in DD neurons, we next investigated if these components might interact with PAL-1. We found that double mutants of *pal-1* and *vang-1* displayed significantly more severe anterior shifts, at one or more DD neuron positions, compared to either single mutant (Fig3A and B). A similar increase was observed in double mutant of *pal-1* and *sax-3.* Both double mutants were comparable to dual loss of *vang-1* and *sax-3*. These results are consistent with a *pal-1* containing pathway acting in concert with *vang-1* and *sax-3* to promote CE during VNC assembly

Mutation of sex-1 produces defects during VNC assembly

Nuclear hormone receptor signalling through members of the retinoic acid receptor family (RARs), ligand induced nuclear receptors, are a key regulator of CDX1/2 (Houle et al., 2003). Retinoic acid signalling, itself, is a prominent determinant of neural tube development and has been shown to affect convergent extension (Mic et al., 2002, Wilson et al., 2003; Kam et al., 2013; Gur et al., 2022). Along with *zy43* and *zy44*, we also identified a mutation in an orphan

nuclear hormone receptor, *sex-1*, which produces anterior DD neuron shifts. SEX-1 displays some homology to the RAR family, orphan nuclear hormone receptor REV-ERBβ and ROR family (Carmi et al., 1998). To confirm a possible role for *sex-1* in VNC assembly, we used cas9 mediated deletion to generate *zy130*, an allele bearing a 7bp deletion in the first intron of the gene. The alleles produced a high degree of lethality in worm progeny and showed several phenotypes that have previously been attributed to decreased gene transcription of *sex-1*, including vulval defects, movement of the nerve ring and a higher proportion of male worms (data not shown). *zy130* worms also display a significant anterior shift amongst VNC neurons with failed intercalation amongst anterior neurons at a low percentage (Fig4A and B).

While *sex-1* mutants display anterior shifts amongst the majority of their neurons, we also noted the unique DD2/3 defect, which is also present in *pal-1(zy117)* mutants but not *vang-1(tm1422)* or *sax-3(zy5)* mutants. To test for a possible interaction, we produced double knockouts of *pal-1* and *sex-1*. We observed a stark increase in the anterior shifts present in either single mutant, with 4 or 5 DD neurons commonly found within the anterior half of the larvae (Fig4B). This suggests that the two mutants may function in parallel. We also noted the persistent stalled neuron intercalations amongst VNC neurons in larval stages (Fig4D and E). *sex-1* mutants display an increased amount of neuron pairs that remain along the dorso-ventral axis and have not intercalated into a single file. This defect was more striking in *pal-1; sex-1* double mutants, though not statistically significant compared to *sex-1* single mutants. We noted that while *pal-1* single mutants do display some stalled intercalations, they are not significantly increased from WT. This could suggest a unique phenotype that may contribute to the overall enhancement of *pal-1;sex-1* double mutants.

SEX-1 may function upstream of PAL-1 in a Neuron Specific Context

Several canonical nuclear hormone receptor binding motifs flank the upstream regulatory region of *zy117* that we have described, and previous work has shown that the nuclear hormone receptor NHR-2 can bind the region (Kudron et al., 2018). To explore if these may indicate a genetic relationship between the two genes, we investigated expression of PAL-1 in a sex-1(zy130) background and compared the results with those in a WT or *zy117* background (Fig5A). Compared with WT embryos, deletion of the upstream enhancer element has a notable effect on *pal-1* expression in the VNC. This loss of intensity is proportional to the loss of detectible *cnd-1*+ nuclei. In contrast, *cnd-1*- nuclei show only small changes from WT in *pal-1* backgrounds. We were surprised to see that mutation of *sex-1* resulted in the almost complete loss of PAL-1 expression within the VNC denoted by decrease in the number and intensity of *cnd1*+ cells (Fig5B and C). Loss of *sex-1* failed to significantly decrease pal-1 expression in cnd-1- nuclei or expression in mid-VNC DB neurons. A similar result was observed using a transgene that expressed GFP under the control of the pal-1 promoter, suggesting that the effect of *sex-1* is achieved through transcriptional regulation (Fig5D).

Given the differences when analyzing expression compared to epistatic genetic analysis, we wished to further examine interaction between the two genes. Given a regulatory relationship between *sex-1* and *pal-1*, we predicted that overexpressing *pal-1* within the VNC of a *sex-1* mutant may be able to restore downstream function and rescue mutant defects. To facilitate this, we constructed a plasmid bearing the coding region of *pal-1* and drove expression using a VNC specific bar-1 promoter (Maro et al., 2009). The construct was able to rescue *zy117* defects and possessed minimal defects when overexpressed in WT worms (Fig5E-G). When analysed in a

sex-1(zy130) background, we found that defects were partially rescued. This could support a hypothesis that while *pal-1* is downstream of *sex-1*, it is only one of potentially several targets.

Discussion

Mammalian CDX family members integrate multiple signalling pathways to regulate nervous system development through collective cell movements. Several of these factors play important roles in neurulation and their action through CDX members is thought to be critical to the process (Keenan et al., 2006; Savory et al., 2011; Kam et al., 2013). In support of this, loss of both CDX1 and CDX2, which share a core set of redundant functions, results in a severe form of NTD, crainiosachis, and lethality (Savory et al., 2011; Zhao et al., 2014). Association of the *C. elegans* homolog *pal-1* with severe defects in VNC assembly suggests some of this role for caudal genes is conservation. At present, it is unclear how much of these roles are conserved across species. PAL-1 research in *C. elegans* has primarily focused on cell fate decisions and has been limited to the developing epithelium. Additionally, it is difficult to ascertain how much of its role in PCP signalling is conserved as *C. elegans* lack a PTK7 homolog. In this study, we show that PAL-1 is required for successful intercalation during the mid to late stages of ventral nerve cord assembly facilitated by nuclear hormone receptor signaling.

Complete loss of PAL-1 leads to embryonic lethality due to failures embryonic cell morphogenesis and improper cell fate determination (Edgar et al., 2001). Tissue-specific loss of PAL-1 in the VNC results in the migration and positioning amongst all three sub-type populations of VNC motor neurons but worms are otherwise phenotypically normal. Consistent with roles that have been previously described for PCP components and other proteins which function during embryonic VNC assembly, *pal-1* mutants show severe anterior shifts in neuron positions post-hatching. Given that the defects are not the result of incorrect cell fates, this suggests that in addition to roles in epidermal morphogenesis and cell fate, the function of *pal-1* extends to a role in VNC assembly.

VNC defects observed in *pal-1* mutants bear similarity to those described in embryonic epithelial or intestinal cells (Edgar et al., 2001; Gilbert et al., 2020). Upon tissue-specific loss of the *pal-1* in P and V cells, for example, migration and intercalation movements required for correct cell organisation and junctional formation during late embryogenesis fails (Gilbert et al., 2020). This results in mis-polarization and branching defects in seam cells post hatching. Similarly, early descriptions of *pal-1* and its mutation showed that several embryonic Ms and AB cell lineages, include those that lack WT protein expression, display morphogenetic defects (Edgar et al., 2001). Given that the mechanisms associated with the regulation of intercalation and migration shared with common targets, this likely indicates a broader role for *pal-1*. Limited research has examined the effects of *pal-1* loss on downstream targets, however given the broader role for morphogenic movements a previous screen for targets in the C cell lineage may present some targets (Baugh et al., 2005). Amongst these targets, *nhr-25*, *nhr-60*, *ceh-16* and *mab-21* have been shown to regulate morphogenetic processes during embryogenesis (Chow et al., 1995; Chen et al., 2004; Cassata et al., 2005; Baugh et al., 2005; Simeckova et al., 2007). The *tbx-8*, *tbx-9*, *vab-7* complex may be of interest due to the involvement of adherens junctions which play roles during convergent extension (Pocock et al., 2004; Sawyer et al., 2011).

The action of CDX proteins during neurulation requires, at least in-part, the function of the PCP pathway (Savory et al., 2011). Heterozygous CDX loss genetically compliments the loss of Scribble and another core protein, PTK7, is directly induced by CDX1/2. Our lab has

previously used VNC development in epistatic analysis showing that the severity of defects in neuron positions and rosette lifetime is enhanced in *vang-1* and *sax-3* double mutants but not in *vang-1* and *prkl-1* doubles mutants (Shah et al., 2017). Here we have shown that both larval cell position defects and delays in rosette lifetime are enhanced suggesting that PAL-1 does not act solely through the PCP pathway, as it does in mammals.

Transcriptional enhancers and suppressors play roles in establishing complex spatial and temporal patterns of protein expression needed to facilitate diverse processes (Ong and Corces, 2011; Panigrahi and O'Malley, 2021). Their action requires equally complex regulatory regions, which can support a range of mechanisms. Consistent with this diversity, regulatory regions can display flexibility in their placement relative to their gene, variations in length and composition, and respond to diverse classes of proteins, including chromatin modifiers, transcription factors and enhancer RNA (Frankel, 2012; Li and Wunderlich, 2017; Arnold et al., 2020). PAL-1 is a central hub for signalling pathways within multiple tissues and is widely required for morphogenesis and cell-fate decisions predominantly during embryogenesis, consistent with the lethality of *pal-1* null mutants. To facilitate these wide-reaching roles several studies have shown that various transcription factors and enhancer regions are critical for various roles. From early in development through late embryogenesis, PAL-1 is expressed in C lineage descendants (Edgar et al., 2001). In later stages, its expression expands to include several AB and Ea lineage cells. This expression of the protein is lost post-hatching, except for a limited number of hypodermal tail cells. Gilbert et al., (2005) identified an enhancer in exon 5 that is required for expression of *pal-1* in posterior epithelial cells. Regulation of PAL-1 within the early embryo requires MEX-3 and SKN-1, while suppression in the adult gonad through GLD-1 and PUF-8 binding to a germline recessive element in the 3'UTR (Hunter and Kenyon, 1996; Mootz et al., 2004; Mainpal et al., 2011). Thus, while several specific regions are required for proper expression of *pal-1*, they all fall within the gene or immediately adjacent. For the first time, we have identified a region ~10kb upstream of the start site, which is required for expression of *pal-1* in the DD and DA lineages. Similar regulatory regions and expression patterns have been characterised in mammalian CDX genes. Expression of the gene family commences in the primitive streak and tail bud early during post-implantation before expanding to neuroectoderm and mesodermal tissues, finally decreasing by late gestation (Meyer and Gruss, 1993; Beck et al., 1995; Benahmed et al., 2008). Throughout this dynamic pattern, family members are expressed along the anterior-posterior axis in a nested fashion (Chawengsaksophak et al., 1997). The initiation, maintenance and positioning amongst multiple CDX proteins requires diverse mechanisms including autoregulation, traditional signalling cascades, the paired-box gene PAX3, GATA6, Tcf4 and HNFa (Houle et al., 2003; Beland et al., 2004; Chang et al., 2016; Benahmed et al., 2008; Zhao et al., 2014). These factors, in tern, require a range of regulatory regions, including those several kb from the transcriptional start site (Wang and Shashikant, 2007; Benahmed et al., 2008).

Expression of *pal-1* in the posterior DB neurons is largely unaffected, suggesting that an additional region is needed for such expression. The failure of an extrachromosomal promoter bearing the full upstream region to express *pal-1* in DB neurons suggests that further investigation into additional intergenic or more distal regions may be required. This difference is curious, given that DA/DD neurons consist of different neuron subtypes, while DB neurons share characteristics with DA neurons. The difference may instead reflect the participation of the

different neuron population in different morphogenetic movements, DA/DD neurons participate in CE while DB neurons radially intercalate into the developing VNC at a later stage.

Surprisingly, loss of the nuclear hormone receptor SEX-1 has a significant impact on PAL-1 expression within the VNC during embryonic morphogenesis. SEX-1 is one of several orphan nuclear hormone receptors, which lack a known ligand. It primarily functions during sex determination as an X-chromosomal element to regulation of the transcription factor *xol-1* (Reviewed in Meyer et al., 2010; Farboud et al., 2013). While few other functions have been ascribed to SEX-1, the nuclear hormone receptor superfamily in nematodes contains several members with roles during embryogenesis. The include the *din-1L*, *nhr-25*, *nhr-40* and *nhr-60* (Asahina et al., 2000; Ludewig et al., 2004; Brozova et al., 2006; Simeckova et al., 2007).

In the context of convergent extension and neurulation, the homology between *sex-1* and the retinoic acid receptor family (Carmi et al., 1998), is of particular importance. Retinoic acid has been shown to regulate CDX1 expression through its receptor, with loss of regulatory regions leading to decreased expression of the protein around timepoints when neurulation is underway (Houle et al., 2003). Genetic disruption of retinoic acid signalling is sufficient to induce defects in convergent extension (Kam et al., 2013; Gur et al., 2022). This homology also extends to several other groups of NHRs, including REV-ERBβ, orphan retinoic acid receptor-related orphan receptor (ROR) subfamily and the orphan NHR E78A, in *Drosophila* (Carmi et al., 1998). These additional families have well described roles in development and the nervous system, however few direct connections with the collective cell movements during neurulation have been described. REV-ERBβ, for example, displays prominent expression in the floor of the neural tube and developing nervous system but functions largely in the circadian clock molecular circuit (Bonnelye et al., 1994; Ikeda et al., 2019). RORα is prominently found in developing ganglion cells in the cerebellum (Gold et al., 2003). This novel role for *sex-1* is also surprising given that few functions for the gene have been described outside of its prominent role in determination of nematode sex through the master regulator *xol-1* (Carmi et al., 1998; Farboud et al., 2013). While the interaction between SEX-1 and *xol-1* involves nuclear hormone receptor binding motifs like those found near the *pal-1* upstream regulatory region, the well-defined action of SEX-1 is to repress *xol-1* (Farboud et al., 2013). This would suggest that the receptor may have additional functions which remain to be identified. Non-canonical roles have been reported for other components of sex determination, including in growth and metabolism (Dumas et al., 2013; Webster et al., 2013). Further investigation will be needed to clarify if the interaction is direct or mediated through another transcription factor.

This study has explored the role and regulation of the CDX family homolog *pal-1* during VNC assembly in *C. elegans*. Given the prominent role that CDX family members during embryonic development in the neural tube and other mesodermal tissues, it is important to understand the mechanisms that influence their role and what functions are conserved across species.

Materials and Methods

Strains and Maintenance

All strains were maintained and examined at 20ºC. The Bristol N2 strain was used as wild type (WT), along with the following alleles and transgenes: LGII: *unc-4(syb1658[unc-4::GFP]).* LGIII: *pal-1(zy43), pal-1(zy44), pal-1(zy117)*. LGX: *sex-1(zy45), sex-1(zy130), sex-1(zy159),*

sax-3(zy5), vang-1(tm1422), zyIs36[cnd-1p::PH::mCherry myo-2p::mCherry]. Unassigned linkage: OU792, OU734, *zyIs40[unc-30p::gfp; cnd-1p::PH::mCherry myo-2p::mCherry]*.

pal-1 and *sex-1* mutant alleles

pal-1(zy43), pal-1(zy44) and *sex-1(zy45)* were identified in a genetic screen for DD neuron position defects (A. Colavita, unpublished). Whole-genome sequencing, as described in Noblett et al. (2019), was used to identify the genes and their associated DNA lesions. Mutants were subsequently outcrossed at least three times and reverified by Sanger sequencing (performed at OHRI StemCore) using primers N35-N36 for *pal-1* and N39-N40 for *sex-1* (all primers listed in Supplemental Table 1).

The *pal-1(zy117)* deletion was generated via DNA repair of CRISPR-Cas9-induced double strand breaks (Waaijers et al., 2013). Briefly, the target site (GAATGTCATAATGACCTTTT) was identified using the IDT guide RNA design tool at idtdna.com. The sequence was inserted into the Cas9-sgRNA plasmid pDD162 (Addgene #47549) using the NEB Q5 Site-Directed Mutagenesis Kit to generate plasmid pAC564. Young adult worms containing the DD reporter transgene *ynIs37* were injected with a mix of 50 ng/µl of pAC564, 2.5 ng/µl of myo-2p::mCherry (pCFJ90, Addgene #19327) and pBluescript plasmid (Stratagene) to a concentration of 100 ng/µl. Progeny were screened for DD position defects that resembled those in *zy43* and *zy44*. Sequencing (OHRI StemCore) with primers N35 and N36 was used to identify the deletion. Subsequent genotyping was performed using primers N35-N37.

The *sex-1(zy130)* deletion was generated using CRISPR-Cas9 and identified by screening for DD position defects in a similar manner. The Cas9-sgRNA plasmid (pAC683) contained the target site sequence CAATGGTCACATCTTCCGAC. Sequencing (OHRI StemCore) with primers N39 and N40 was used to identify the deletion.

CRISPR-Cas9-mediated knock-ins

A GFP::3xFLAG and an mNG::AID::3xFLAG were inserted at the C-terminus of the endogenous *pal-1* and *sex-1* loci, respectively, using the CRISPR-Cas9 self-excising drug selection cassette approach described in Dickinson et al. (2015). Target sequences for *pal-1* (GTCGTGACAAACAGAAGATT) and *sex-1* (CAAAGGTGGCTAGCAGTGAA) insertions were cloned into the Cas9–sgRNA plasmid pDD162 to generate plasmids pAC487 and pAC703, respectively. The homology directed repair plasmids for *pal-1* (pAC486) and *sex-1* (pAC722) were constructed using the GFP (pDD282, Addgene #66823) and mNG::AID (pJW1582, Addgene #154312) selection cassette plasmids, respectively. The resulting knock-in alleles are *pal-1(zy112[pal-1::GFP])* and *sex-1(zy133[sex-1::mNG::AID])*.

Reporter and rescue constructs

A *pal-1p::mNG* transcriptional reporter (pAC499) was constructed using Gibson Assembly (New England Biolabs). This reporter combines approximately 1.8 kb of distal and 2.4 kb of proximal promoter elements upstream of an mNG cassette, with the pPD95.77 vector (a gift from Andrew Fire, Stanford) serving as the backbone. Primers N51-N56 were used for the assembly (Table S1).

A promoterless *pal-1::GFP* minigene plasmid (pAC936) was constructed using Gibson Assembly. This construct contains the *pal-1* genomic coding region, with introns 3 and 5 removed, fused to the *GFP::3X Flag* cassette from the endogenous knock-in allele *pal-1*(zy112). Primers N57-N64 were used for the assembly (Table S1). The *bar-1p::pal-1::GFP* rescue construct (pAC937) was made by inserting a 4.9 kb *bar-1* promoter into pAC936 using Gibson Assembly with primers N65 and N68 (Table S1).

pAC499 and pAC936 were each injected at a concentration of 5 ng/µl, along with 2.5 ng/µl of *myo-2p::mCherry* (pCFJ90) and 92.5 ng/µl of pBluescript plasmid.

Embryonic Imaging

For widefield imaging, embryos were transferred from plates using a capillary attached to a glass pipette and mounted in a 3 µL drop of M9 containing approximately fifty 25 µm diameter polystyrene beads (Polyscience Inc.). The preparation was then sealed under a No. 1.5 coverslip using Vaseline. All widefield imaging was conducted on a Zeiss Imager M2, equipped with a Zeiss SVB-1 microscope signal distribution box/*TTL* trigger cable-controlled camera shutter to reduce phototoxicity. Single time-point images were taken across 15-30 0.5 µm slices at 63x (1.4NA). Unless otherwise stated, all images were deconvolved prior to analysis using constrained iterative deconvolution on Zen 3.2 (Zeiss) with a Gaussian algorithm, corrections for background and saturated pixels.

Embryonic imaging for intensity measurements were acquired on a DM16000B Quorum Spinning Disk (Leica) with a EMCCD (Hamamatsu). Single time-point images were taken at 63x (1.4NA) with a pinhole size of 50um. Images were acquired with a Brightfield exposure of 223ms, at FITC exposure of 500ms and a Cy3 exposure of 700ms, across 12 0.5um slices.

Quantification of motor neuron position defects in newly hatched larvae

Quantification of neuron position defects in L1 larvae was performed as follows. First stage larvae (L1) were mounted on 2% agarose pads using 200 µM levamisole (#31742, Sigma). Images were acquired using a Zeiss Imager M2, Colibri7 LED source, AxiocamHR camera and taken at 40x (1.4NA) over 5-7 0.5um slices. Brightfeild, RFP and GFP channels were acquired. Images were measured on FIJI/Image J software, version 2.14. Using the segmented line tool, the position of each DD, DA and DB neuron (or only DD and DA neurons in OU734) was measured along the worm. These positions were then converted into percentage locations using SABVR = 0% and the anus = 100%. Each percentage location was plotted using base R, version 4.4.2 (R Core Team, 2019) and geom_jitter from the ggplot2 suite (Wilkinson, 2011).

Quantification of PAL-1 expression

Intensity measurements of *pal-1(zy112[pal-1::GFP])* and *sex-1(zy133[sex-1::mNG::AID])*were conducted using Imaris 10 (Bitplane) after data was processed using Fiji/ImageJ. Briefly, Z-stacks were opened in their native format in Fiji/ImageJ. Both red and green channels were merged to form a composite color image, which was converted into RGB before exporting as a TIFF. Data was then imported into Imaris. Semi-automated spot detection was used to identify GFP nuclei with a XY diameter of at least 1.15 µm and a quality above 42. Spots were classified using the Imaris machine learning tool based upon the RFP channel and their proximity to the RFP labelled VNC cells. After spot creation was complete, the original GFP image was used to remove false positive spots which were outside the embryo boundary.

Spots details including class and SUM Intensity were exported for statistical analysis and graphing.

Statistics

Larval and embryo measurements were compared across populations with the indicated number of individuals shown in each figure. Two-tailed t-tests or ANOVA were used to calculate p values between control and treatment groups, determined by the number of treatments, using base R, version 4.4.2 (R Core Team, 2019) and the multicomp package (Bretz et al., 2011). Measurements related to embryonic phenotypes (expression pattern and order measurements) were scored blind to genotype using the Blind Analysis Tools plugin for Fiji/ImageJ (https://imagej.net/plugins/blind-analysis-tools).

Acknowledgements

We thank Chris Li for sharing *ynIs37*. Some strains were provided by the *Caenorhabditis* Genetics Center, which is funded National Institutes of Health Office of Research Infrastructure Programs (P40 OD010440). Data for *C. elegans* allele sequences was accessed through WormBase (http://www.wormbase.org, release WS294). The authors acknowledge the Cell Biology and Image Acquisition Core (RRID: SCR_021845) funded by the University of Ottawa, Natural Sciences and Engineering Research Council of Canada, and the Canada Foundation for Innovation. We would also like to acknowledge the assistance of StemCore Laboratories Genomics Core Facility (OHRI), RRID:SCR_012601. Studies presented in this report were supported by a Canadian Institutes of Health Research Project Grant (FRN 156160) to A. Colavita.

Author Contributions

N.N preformed experiments and data analysis. T.R preformed molecular biology procedures. S.F preformed sequence analysis. N.N and A.C wrote the manuscript. A.C supervised the research.

Declarations

The authors declare no competing interests.

References

Arnold, P. R., Wells, A. D., & Li, X. C. (2020). Diversity and emerging roles of enhancer RNA in regulation of gene expression and cell fate. *Frontiers in cell and developmental biology*, *7*, 377.

Asahina, M., Ishihara, T., Jindra, M., Kohara, Y., Katsura, I., & Hirose, S. (2000). The conserved nuclear receptor Ftz-F1 is required for embryogenesis, moulting and reproduction in Caenorhabditis elegans. *Genes to Cells*, *5*(9), 711-723.

Baugh, L. R., Hill, A. A., Claggett, J. M., Hill-Harfe, K., Wen, J. C., Slonim, D. K., ... & Hunter, C. P. (2005). The homeodomain protein PAL-1 specifies a lineage-specific regulatory network in the C. elegans embryo.

Beck, F., Erler, T., Russell, A., & James, R. (1995). Expression of Cdx-2 in the mouse embryo and placenta: possible role in patterning of the extra-embryonic membranes. *Developmental Dynamics*, *204*(3), 219-227.

Belakavadi, M., & Fondell, J. D. (2006). Role of the mediator complex in nuclear hormone receptor signaling. *Reviews of physiology, biochemistry and pharmacology*, 23-43.

Béland, M., Pilon, N., Houle, M., Oh, K., Sylvestre, J. R., Prinos, P., & Lohnes, D. (2004). Cdx1 autoregulation is governed by a novel Cdx1-LEF1 transcription complex. *Molecular and cellular biology*, *24*(11), 5028-5038.

Benahmed, F., Gross, I., Gaunt, S. J., Beck, F., Jehan, F., Domon–Dell, C., ... & Duluc, I. (2008). Multiple regulatory regions control the complex expression pattern of the mouse Cdx2 homeobox gene. *Gastroenterology*, *135*(4), 1238-1247.

Bonnelye, E., Vanacker, J. M., Desbiens, X., Begue, A., Stehelin, D., & Laudet, V. (1994). Rev-erbb, a new member of the nuclear receptor superfamily, is expressed in the nervous system during chicken development. *Cell Growth and Differentiation-Publication American Association for Cancer Research*, *5*(12), 1357-1366.

Bretz F, Hothorn T, Westfall PH. Multiple comparisons using R. Boca Raton, FL: CRC Press; 2011.

Brožová, E., Šimečková, K., Kostrouch, Z., Rall, J. E., & Kostrouchová, M. (2006). NHR-40, a Caenorhabditis elegans supplementary nuclear receptor, regulates embryonic and early larval development. *Mechanisms of development*, *123*(9), 689-701.

Carmi, I., Kopczynski, J. B., & Meyer, B. J. (1998). The nuclear hormone receptor SEX-1 is an X-chromosome signal that determines nematode sex. *Nature*, *396*(6707), 168-173.

Cassata, G., Shemer, G., Morandi, P., Donhauser, R., Podbilewicz, B., & Baumeister, R. (2005). ceh-16/engrailed patterns the embryonic epidermis of Caenorhabditis elegans.

Chang, J., Skromne, I., & Ho, R. K. (2016). CDX4 and retinoic acid interact to position the hindbrain–spinal cord transition. *Developmental biology*, *410*(2), 178-189.

Chawengsaksophak, K. (2019). Cdx2 animal models reveal developmental origins of cancers. *Genes*, *10*(11), 928.

Chen, Z., Eastburn, D. J., & Han, M. (2004). The Caenorhabditis elegans nuclear receptor gene nhr-25 regulates epidermal cell development. *Molecular and cellular biology*, *24*(17), 7345-7358.

Chow, K. L., Hall, D. H., & Emmons, S. W. (1995). The mab-21 gene of Caenorhabditis elegans encodes a novel protein required for choice of alternate cell fates. *Development*, *121*(11), 3615-3626.

Devitt, C. C., Weng, S., Bejar-Padilla, V. D., Alvarado, J., & Wallingford, J. B. (2024). PCP and Septins govern the polarized organization of the actin cytoskeleton during convergent extension. *Current Biology*, *34*(3), 615-622.

Dumas, K. J., Delaney, C. E., Flibotte, S., Moerman, D. G., Csankovszki, G., & Hu, P. J. (2013). Unexpected role for dosage compensation in the control of dauer arrest, insulin-like signaling, and FoxO transcription factor activity in Caenorhabditis elegans. *Genetics*, *194*(3), 619-629.

Edgar, L. G., Carr, S., Wang, H., & Wood, W. B. (2001). Zygotic expression of the caudal homolog pal-1 is required for posterior patterning in Caenorhabditis elegans embryogenesis. *Developmental biology*, *229*(1), 71-88.

Farboud, B., Nix, P., Jow, M. M., Gladden, J. M., & Meyer, B. J. (2013). Molecular antagonism between X-chromosome and autosome signals determines nematode sex. *Genes & development*, *27*(10), 1159-1178.

Frankel, N. (2012). Multiple layers of complexity in cis-regulatory regions of developmental genes. *Developmental Dynamics*, *241*(12), 1857-1866.

Gilbert, S. P., Mullan, T. W., Poole, R. J., & Woollard, A. (2020). Caudal-dependent cell positioning directs morphogenesis of the C. elegans ventral epidermis. *Developmental Biology*, *461*(1), 31-42.

Gold, D. A., Baek, S. H., Schork, N. J., Rose, D. W., Larsen, D. D., Sachs, B. D., ... & Hamilton, B. A. (2003). RORα coordinates reciprocal signaling in cerebellar development through sonic hedgehog and calcium-dependent pathways. *Neuron*, *40*(6), 1119-1131.

Gur, M., Edri, T., Moody, S. A., & Fainsod, A. (2022). Retinoic acid is required for normal morphogenetic movements during gastrulation. *Frontiers in cell and developmental biology*, *10*, 857230.

Hayes, M., Naito, M., Daulat, A., Angers, S., & Ciruna, B. (2013). Ptk7 promotes non-canonical Wnt/PCP-mediated morphogenesis and inhibits Wnt/β-catenin-dependent cell fate decisions during vertebrate development. *Development*, *140*(8), 1807-1818.

Houle, M., Sylvestre, J. R., & Lohnes, D. (2003). Retinoic acid regulates a subset of Cdx1 function in vivo.

Hunter, C. P., & Kenyon, C. (1996). Spatial and temporal controls target pal-1 blastomere-specification activity to a single blastomere lineage in C. elegans embryos. *Cell*, *87*(2), 217-226.

Ikeda, R., Tsuchiya, Y., Koike, N., Umemura, Y., Inokawa, H., Ono, R., ... & Yagita, K. (2019). REV-ERBα and REV-ERBβ function as key factors regulating Mammalian Circadian Output. *Scientific reports*, *9*(1), 10171.

Kam, R. K. T., Shi, W., Chan, S. O., Chen, Y., Xu, G., Bik-San Lau, C., ... & Zhao, H. (2013). Dhrs3 protein attenuates retinoic acid signaling and is required for early embryonic patterning. *Journal of Biological Chemistry*, *288*(44), 31477-31487.

Keenan, I. D., Sharrard, R. M., & Isaacs, H. V. (2006). FGF signal transduction and the regulation of Cdx gene expression. *Developmental biology*, *299*(2), 478-488.

Keller, M. S., Ezaki, T., Guo, R. J., & Lynch, J. P. (2004). Cdx1 or Cdx2 expression activates E-cadherin-mediated cell-cell adhesion and compaction in human COLO 205 cells. *American Journal of Physiology-Gastrointestinal and Liver Physiology*, *287*(1), G104-G114.

Khan, S. H., & Okafor, C. D. (2022). Interactions governing transcriptional activity of nuclear receptors. *Biochemical Society Transactions*, *50*(6), 1941-1952.

Kudron, M. M., Victorsen, A., Gevirtzman, L., Hillier, L. W., Fisher, W. W., Vafeados, D., ... & Waterston, R. H. (2018). The ModERN resource: genome-wide binding profiles for hundreds of Drosophila and Caenorhabditis elegans transcription factors. *Genetics*, *208*(3), 937-949.

Li, L., & Wunderlich, Z. (2017). An enhancer's length and composition are shaped by its regulatory task. *Frontiers in genetics*, *8*, 63.

Lorentz, O., Duluc, I., Arcangelis, A. D., Simon-Assmann, P., Kedinger, M., & Freund, J. N. (1997). Key role of the Cdx2 homeobox gene in extracellular matrix–mediated intestinal cell differentiation. *Journal of Cell Biology*, *139*(6), 1553-1565.

Ludewig, A. H., Kober-Eisermann, C., Weitzel, C., Bethke, A., Neubert, K., Gerisch, B., ... & Antebi, A. (2004). A novel nuclear receptor/coregulator complex controls C. elegans lipid metabolism, larval development, and aging. *Genes & development*, *18*(17), 2120-2133.

Maduro, M. F., Kasmir, J. J., Zhu, J., & Rothman, J. H. (2005). The Wnt effector POP-1 and the PAL-1/Caudal homeoprotein collaborate with SKN-1 to activate C. elegans endoderm development. *Developmental biology*, *285*(2), 510-523.

Mainpal, R., Priti, A., & Subramaniam, K. (2011). PUF-8 suppresses the somatic transcription factor PAL-1 expression in C. elegans germline stem cells. *Developmental biology*, *360*(1), 195-207.

Maro, G. S., Klassen, M. P., & Shen, K. (2009). A β-catenin-dependent Wnt pathway mediates anteroposterior axon guidance in C. elegans motor neurons. *PloS one*, *4*(3), e4690.

Martinez, S., Scerbo, P., Giordano, M., Daulat, A. M., Lhoumeau, A. C., Thomé, V., ... & Borg, J. P. (2015). The PTK7 and ROR2 protein receptors interact in the vertebrate WNT/planar cell polarity (PCP) pathway. *Journal of Biological Chemistry*, *290*(51), 30562-30572.

Mic, F. A., Haselbeck, R. J., Cuenca, A. E., & Duester, G. (2002). Novel retinoic acid generating activities in the neural tube and heart identified by conditional rescue of Raldh2 null mutant mice.

Meyer, B. I., & Gruss, P. (1993). Mouse Cdx-1 expression during gastrulation. *Development*, *117*(1), 191-203.

Meyer, B. J. (2010). Targeting X chromosomes for repression. *Current opinion in genetics & development*, *20*(2), 179-189.

Mootz, D., Ho, D. M., & Hunter, C. P. (2004). The STAR/Maxi-KH domain protein GLD-1 mediates a developmental switch in the translational control of C. elegans PAL-1.

Noblett, N., Wu, Z., Ding, Z. H., Park, S., Roenspies, T., Flibotte, S., ... & Colavita, A. (2019). DIP-2 suppresses ectopic neurite sprouting and axonal regeneration in mature neurons. *Journal of Cell Biology*, *218*(1), 125-133.

Noblett, N., Roenspies, T., Flibotte, S., & Colavita, A. (2024). IPPK-1 and IP6 contribute to ventral nerve cord assembly in C. elegans. *bioRxiv*, 2024-03.

Ong, C. T., & Corces, V. G. (2011). Enhancer function: new insights into the regulation of tissue-specific gene expression. *Nature Reviews Genetics*, *12*(4), 283-293.

Palmer, A. J., Savery, D., Massa, V., Copp, A. J., & Greene, N. D. (2021). Genetic interaction of Pax3 mutation and canonical Wnt signaling modulates neural tube defects and neural crest abnormalities. *Genesis*, *59*(11), e23445.

Panigrahi, A., & O'Malley, B. W. (2021). Mechanisms of enhancer action: the known and the unknown. *Genome biology*, *22*(1), 108.

Pocock, R., Ahringer, J., Mitsch, M., Maxwell, S., & Woollard, A. (2004). A regulatory network of T-box genes and the even-skipped homologue vab-7 controls patterning and morphogenesis in C. elegans.

R Core Team (2019) R: a language and environment for statistical computing. R Foundation for Statistical Computing, Vienna, Austria. https://www.R-project.org

Savory, J. G., Mansfield, M., Rijli, F. M., & Lohnes, D. (2011). Cdx mediates neural tube closure through transcriptional regulation of the planar cell polarity gene Ptk7. *Development*, *138*(7), 1361-1370.

Sawyer, J. K., Choi, W., Jung, K. C., He, L., Harris, N. J., & Peifer, M. (2011). A contractile actomyosin network linked to adherens junctions by Canoe/afadin helps drive convergent extension. *Molecular biology of the cell*, *22*(14), 2491-2508.

Shah, P. K., Tanner, M. R., Kovacevic, I., Rankin, A., Marshall, T. E., Noblett, N., ... & Colavita, A. (2017). PCP and SAX-3/Robo pathways cooperate to regulate convergent extension-based nerve cord assembly in C. elegans. *Developmental cell*, *41*(2), 195-203.

Shindo, A., Inoue, Y., Kinoshita, M., & Wallingford, J. B. (2019). PCP-dependent transcellular regulation of actomyosin oscillation facilitates convergent extension of vertebrate tissue. *Developmental biology*, *446*(2), 159-167.

Šimečková, K. (2007). Nuclear receptors in Caenorhabditis elegans: NHR-60 regulates embryonic development.

Waaijers, S., & Boxem, M. (2014). Engineering the Caenorhabditis elegans genome with CRISPR/Cas9. *Methods*, *68*(3), 381-388.

Wang, W. C., & Shashikant, C. S. (2007). Evidence for positive and negative regulation of the mouse Cdx2 gene. *Journal of Experimental Zoology Part B: Molecular and Developmental Evolution*, *308*(3), 308-321.

Waring, D. A., & Kenyon, C. (1991). Regulation of cellular responsiveness to inductive signals in the developing C. elegans nervous system. *Nature*, *350*(6320), 712-715.

Webster, C. M., Wu, L., Douglas, D., & Soukas, A. A. (2013). A non-canonical role for the C. elegans dosage compensation complex in growth and metabolic regulation downstream of TOR complex 2. *Development*, *140*(17), 3601-3612.

Wehner, P., Shnitsar, I., Urlaub, H., & Borchers, A. (2011). RACK1 is a novel interaction partner of PTK7 that is required for neural tube closure. *Development*, *138*(7), 1321-1327.

Wilkinson, L. (2011). ggplot2: elegant graphics for data analysis by WICKHAM, H.

Wilson, L., Gale, E., & Maden, M. (2003). The role of retinoic acid in the morphogenesis of the neural tube. *Journal of anatomy*, *203*(4), 357-368.

Ybot-Gonzalez, P., Savery, D., Gerrelli, D., Signore, M., Mitchell, C. E., Faux, C. H., ... & Copp, A. J. (2007). Convergent extension, planar-cell-polarity signalling and initiation of mouse neural tube closure.

Zhu, Y., & Lohnes, D. (2022). Regulation of axial elongation by Cdx. *Developmental Biology*, *483*, 118-127.

Zhao, T., Gan, Q., Stokes, A., Lassiter, R. N., Wang, Y., Chan, J., ... & Zhou, C. J. (2014). β-catenin regulates Pax3 and Cdx2 for caudal neural tube closure and elongation. *Development*, *141*(1), 148-157.

Zhao, T., McMahon, M., Reynolds, K., Saha, S. K., Stokes, A., & Zhou, C. J. (2022). The role of Lrp6-mediated Wnt/β-catenin signaling in the development and intervention of spinal neural tube defects in mice. *Disease models & mechanisms*, *15*(6), dmm049517.

Data availability

Data will be made available upon request.

Figure Legends

Table 1: Key Resources

Reagent or resource	Source	Identifier
Chemicals, Peptides, and Recombinant Proteins		
Phytic acid sodium salt hydrate	Sigma-Aldritch	P0109; CAS:14306-25-3
Levamisol hydrochloride	Millipore Sigma	31742; CAS:16595-80-5
Bacterial and Virus Strains		
E. coli: OP50	Caenorhabditis Genetics Center (CGC)	RRID: WB-STRAIN:WBStrain00041969
Experimental Models: Organisms/Strains		
C. elegans: N2 (wild isolate)	CGC	
C. elegans: OU792 (unc-4(zy123[unc-4::mNG]) zySi2[unc-30p::mcherry::H2B::unc-30]; vab-7(zy142[vab7::mNG::T2A::mScarlet-i::H2B])	Antonio Colavita	N/A
C. elegans: OU734 (unc-4(zy123[unc-4::mNG]) zySi2[unc-30p::mcherry::H2B::unc-30])	Antonio Colavita	N/A
C. elegans: *pal-1(zy43)* III	This study	N/A
C. elegans: *pal-1(zy44)* III	This study	N/A
C. elegans: *pal-1(zy117)* III	This study	N/A

C. elegans: *sex-1(zy130) X*	This study	N/A
C. elegans: *pal-1(zy112[pal-1::GFP])* III	This study	N/A
C. elegans: *sex-1(zy133[zy133[sex-1::mNG::AID])* X	This study	N/A
C. elegans: *ynIs37[flp-13p::gfp]* III	CGC	WB Strain: NY2037; WormBase: WBStrain00029158
C. elegans: *sax-3(zy5) X*	Shah et al., 2017	N/A
C. elegans: *vang-1(ok1142) X*	CGC	WB Strain: RB1125; WormBase: WBStrain00031829
C. elegans: *zyIs36(cnd-1::PH::mCherry; myo-2p::mCherry) X*	Antonio Colavita, Shah et al., 2017	N/A
C. elegans: *zyIs40(unc-30p::gfp; cnd-1::PH::mCherry)* Unassigned linkage	This study	N/A
Oligonucleotides		
DNA Oligonucleotides	Eurofins	See Table S1 for sequences and use.
Software and Algorithms		
Zeiss Zen 3.2	Zeiss	https://www.zeiss.com/microscopy/en/products/software/zeiss-zen.html
R 4.4.2	R Core Team, 2019	N/A
Ggplot2	Wickham (2016)	https://github.com/tidyverse/ggplot2
Imaris 10	Oxford Instruments	https://imaris.oxinst.com/

Figure 1: A distal element promotes pal-1 expression in VNC neurons. (A) Representative images of DD positions in WT, *pal-1(zy43)* and *pal-1(zy44)* mutants, identified in a forward genetic screen, visualised using the DD-specific *flp-13p::GFP* reporter. Green arrowheads mark DD neurons, the white arrowhead marks the anus. Scale bar = 20µm. (B) Diagram of pal-1 genomic region showing the positions of mutations used in this study. (C) Representative maximum projections of an endogenous *pal-1p::pal-1::GFP* reporter at three stages of embryonic development. Nomarski image indicates the morphology of the embryo. A cnd-1p::RFP::PH reporter shown in magenta highlights DD and DA neurons around the midline of the embryo. Scale bar = 10µm. (D) Representative images shown pal-1p::PAL-1::GFP in a WT

and *zy117* mutant background. The dotted line indicates areas of interest with expression changes between the two genetic backgrounds Scale bar = 10μm.

Figure 2: pal-1 is involved in motor neuron spacing in the VNC. (A) Representative images of WT and *pal-1(zy117)* in a OU792 background. DA neurons are indicated in green, DB neurons in grey and DD neurons in magenta. Magenta arrowheads mark the position of DD neurons, the white arrowhead marks the anus. Scale bar = 20μm. (B) Quantification of DD and DA neuron position relative to the SABVL neuron in L1 stage worms. Neurons are plotted along the AP axis, where SABVL and anus mark the 0% and 100% positions respectively. Means and 95% confidence intervals are indicated for each neuron and animals scored (N) indicated on the right. Hashed lines indicate the position of WT DD neurons. Significance was determined using a one-way ANOVA with Tukey's post-hoc test, only neurons with a p-value of above 0.05 compared to WT are shown on the graph. Colored arrows show significant shifts of each neuron type from the position of their WT equivalent. *p<0.05, **p<0.01, ***p<0.001. (C) Schematic of the WT neuron order of the larval VNC. DA neurons in green and DD neurons in magenta. (D) Quantification of the order of DA, DB and DD neurons in WT and pal-1(zy117) worms. Individual boxes show the identity of the neuron in each position along the VNC post-hatching with each row indicating an individual. The WT order of neurons is shown above. Significance was determined using a Mann Whitney U-Test. *p<0.05, **p<0.01, ***p<0.001.

Figure 3: pal-1 does not function through the planar cell polarity pathway in C. elegans (A) Representative images of WT, *pal-1(zy117)*, *vang-1(tm1422)*, and *pal-1; vang-1* doubles showing DA neurons in green and DD neurons in magenta. Magenta arrowheads mark the position of DD neurons, the white arrowhead marks the anus. Scale bar = 20μm. (B) Quantification of DD and DA neuron position relative to the SABVL neuron in L1 stage worms. Neurons are plotted along the AP axis, where SABVL and anus mark the 0% and 100% positions respectively. Means and 95% confidence intervals are indicated for each neuron and animals scored (N) indicated on the right. Hashed lines indicate the position of WT DD neurons. Significance was determined using a one-way ANOVA with Tukey's post-hoc test, only neurons with a p-value of above 0.05 compared to WT are shown on the graph. Colored arrows show significant shifts of each neuron type from the position of their WT equivalent. *p<0.05, **p<0.01, ***p<0.001.

Figure 4: PAL-1 expression in the VNC is partially regulated by SEX-1. (A) Representative images of WT, *pal-1(zy117)*, *sex-1(zy130)*, and *pal-1; sex-1* doubles showing DA neurons in green and DD neurons in magenta. Magenta arrowheads mark the position of DD neurons, the white arrowhead marks the anus. Scale bar = 20μm. (B) Quantification of DD and DA neuron position relative to the SABVL neuron in L1 stage worms. Neurons are plotted along the AP axis, where SABVL and anus mark the 0% and 100% positions respectively. Means and 95% confidence intervals are indicated for each neuron and animals scored (N) indicated on the right. Hashed lines indicate the position of WT DD neurons. Significance was determined using a one-way ANOVA with Tukey's post-hoc test, only neurons with a p-value of above 0.05 compared to WT are shown on the graph. Colored arrows show significant shifts of each neuron type from the position of their WT equivalent. (C) Schematic showing the relative position of DD and DA

neurons along the length of the worm. Except for SABD and DA8/9, all neurons have intercalated into a single file by the time of hatching. (D) Representative images of anterior DA and DD neurons in *pal-1(zy117)*, *sex-1(zy130)* and *pal-1; sex-1* double mutants. Asterisks mark neuron pairs that have failed to resolve into a single file. Scale bar = 20µm. (E) Quantification of pairs of neurons that have failed to resolve in larvae. *p<0.05, **p<0.01, ***p<0.001.

Figure 5. SEX-1 is involved in motor neuron spacing. (A) Representative maximum projection images of PAL-1::GFP in WT, pal-1 and sex-1 mutant embryos at lima bean and 1.5-Fold stage. A cnd-1::PH::RFP reporter highlights the cell membranes of neurons, including the DA and DD neurons of the VNC. White circles indicate areas with altered expression in mutant embryos. (B) Quantification of the mean intensity for *PAL-1::GFP* in WT, *pal-1*, and *sex-1* mutant embryos. Measurements were classified based on their co-expression with cnd-1+ cells, labelling the VNC. Means and 95% confidence intervals are indicated for each population with individual measurements shown. (C) Quantification of the number of cells expressing PAL-1::GFP in WT, pal-1 and sex-1 mutant embryos. Cells were classified based on their co-expression with cnd-1+ cells, labelling the VNC. (D) Representative images showing PAL-1p::GFP in a WT or sex-1(zy130) background. Arrows indicate regions of interest. (E) Representative images of DD neurons in *pal-1* and *sex-1* mutants which either express or do not express a *bar-1p::PAL-1::GFP* extrachromosomal transgene. Magenta arrowheads mark the position of DD neurons, the white arrowhead marks the anus. Scale bar = 20µm. (F and G) Quantification of DD neuron position relative to the SABVL neuron in L1 stage worms with or without the extrachromosomal transgene. Neurons are plotted along the AP axis, where SABVL and anus mark the 0% and 100% positions respectively. Means and 95% confidence intervals are indicated for each neuron and animals scored (N) indicated on the right. Hashed lines indicate the position of WT DD neurons. Significance was determined using a two-tailed T-test, only neurons with a p-value of above 0.05 compared to WT are shown on the graph. Colored arrows show significant shifts of each neuron type from the position of their non-transgene equivalent

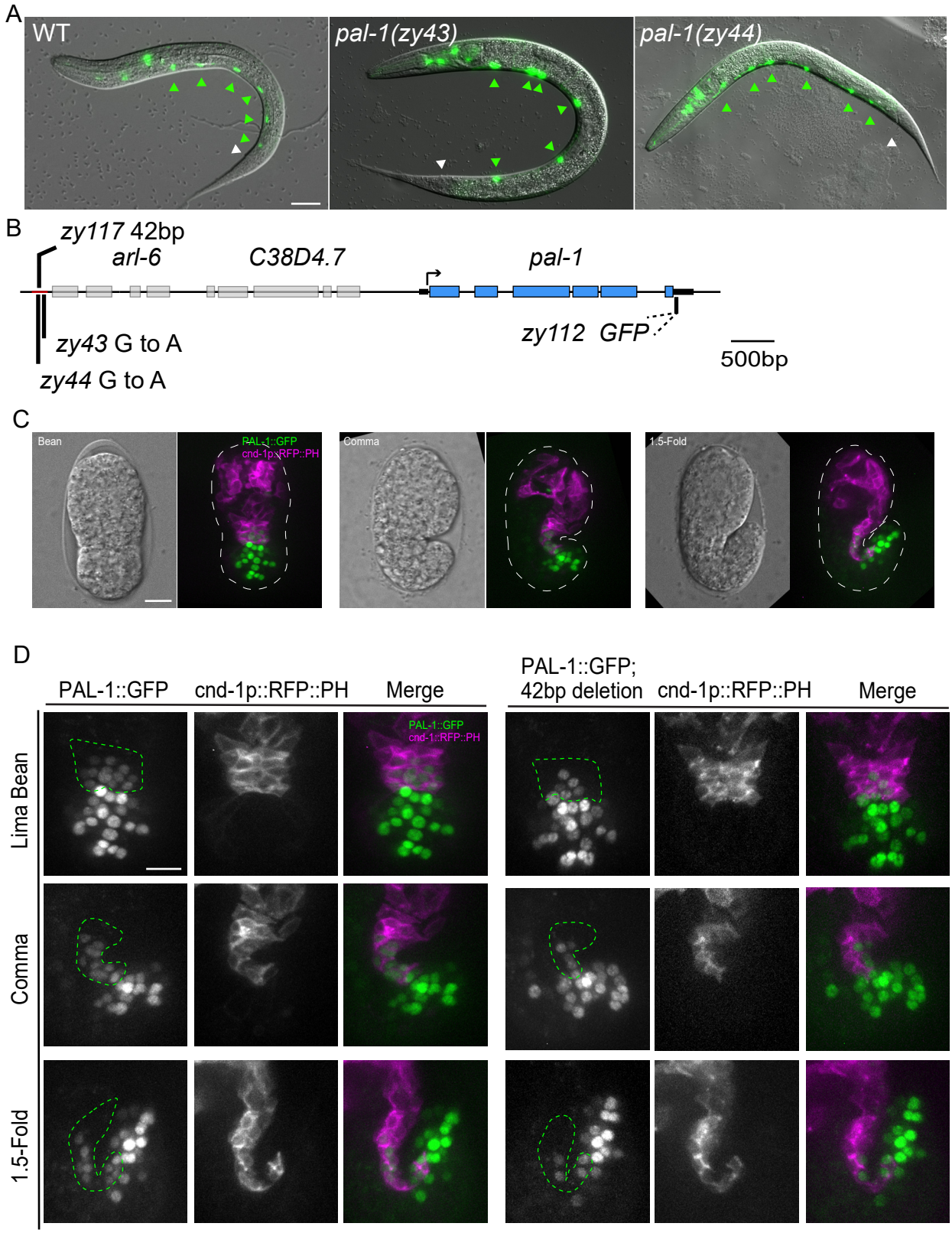
A
WT
pal-1(zy43)
pal-1(zy44)
B
zy117 42bp
arl-6
C38D4.7
pal-1
zy43 G to A
zy44 G to A
zy112 GFP
500bp
C
Bean
PAL-1::GFP
cnd-1p::RFP::PH
Comma
1.5-Fold
D
D
PAL-1::GFP
cnd-1p::RFP::PH
Merge
PAL-1::GFP;
42bp deletion
cnd-1p::RFP::PH
Merge
Lima Bean
Comma
1.5-Fold

FIG 1

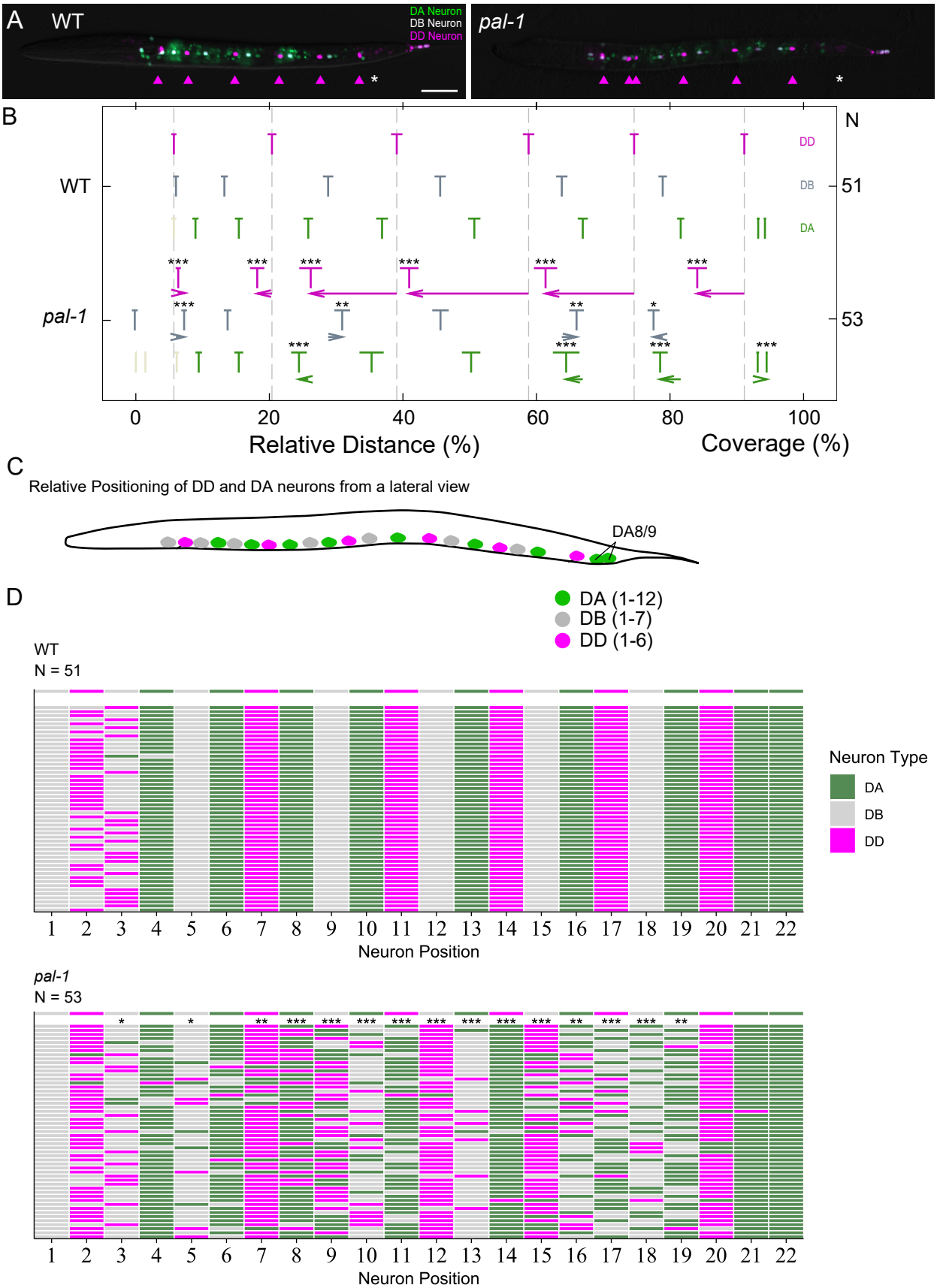
A
WT
DA Neuron
DB Neuron
DD Neuron
pal-1
B
N
WT
pal-1
DD
DB
DA
51
53
0
20
40
60
80
100
Relative Distance (%)
Coverage (%)
C
Relative Positioning of DD and DA neurons from a lateral view
DA8/9
D
DA (1-12)
DB (1-7)
DD (1-6)
WT
N = 51
Neuron Type
DA
DB
DD
Neuron Position
pal-1
N = 53
Neuron Position

FIG 2

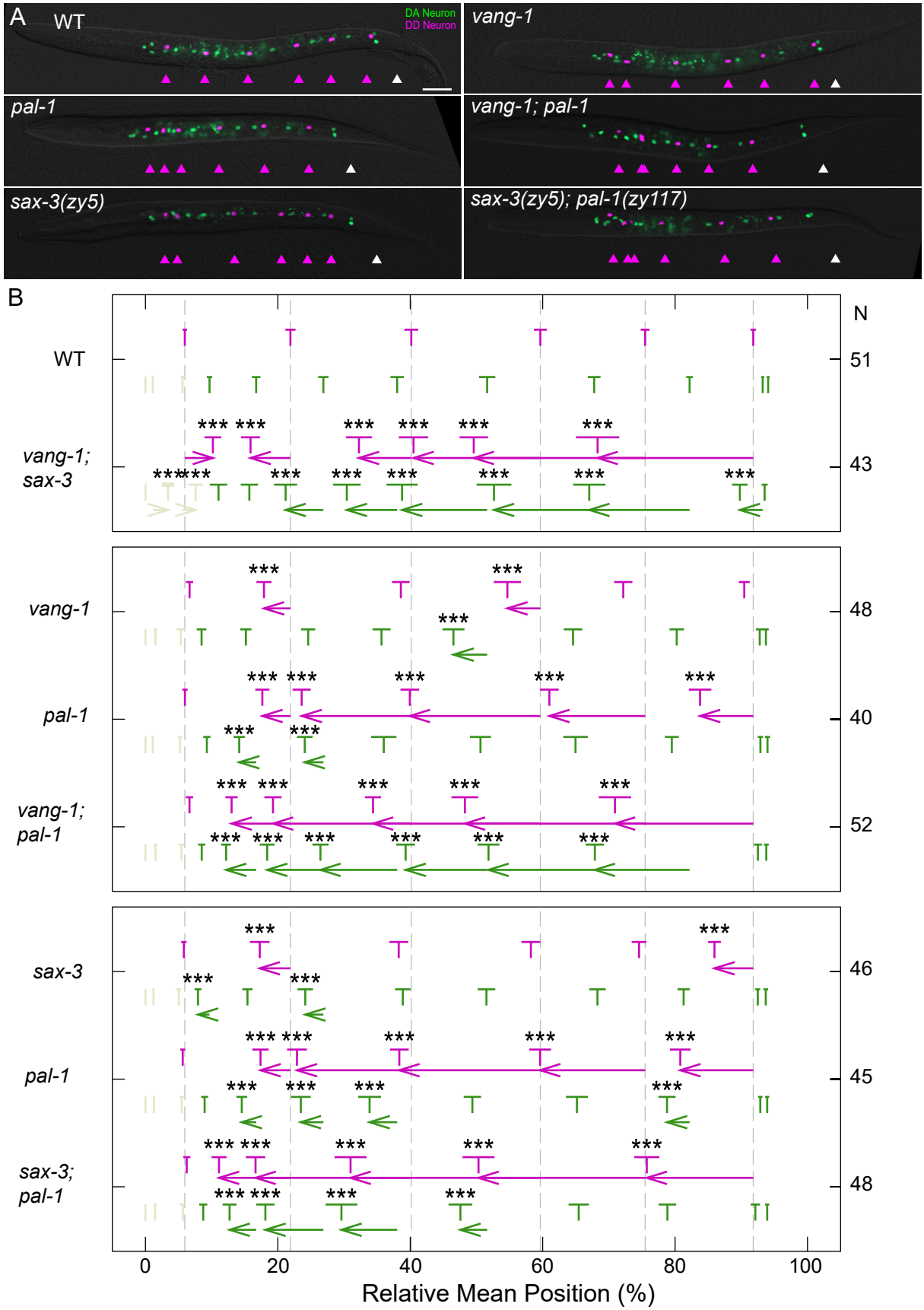
A
WT
DA Neuron
DD Neuron
vang-1
pal-1
vang-1; pal-1
sax-3(zy5)
sax-3(zy5); pal-1(zy117)
B
N
WT
51
vang-1; sax-3
43
vang-1
48
pal-1
40
vang-1; pal-1
52
sax-3
46
pal-1
45
sax-3; pal-1
48
0
20
40
60
80
100
Relative Mean Position (%)

FIG 3

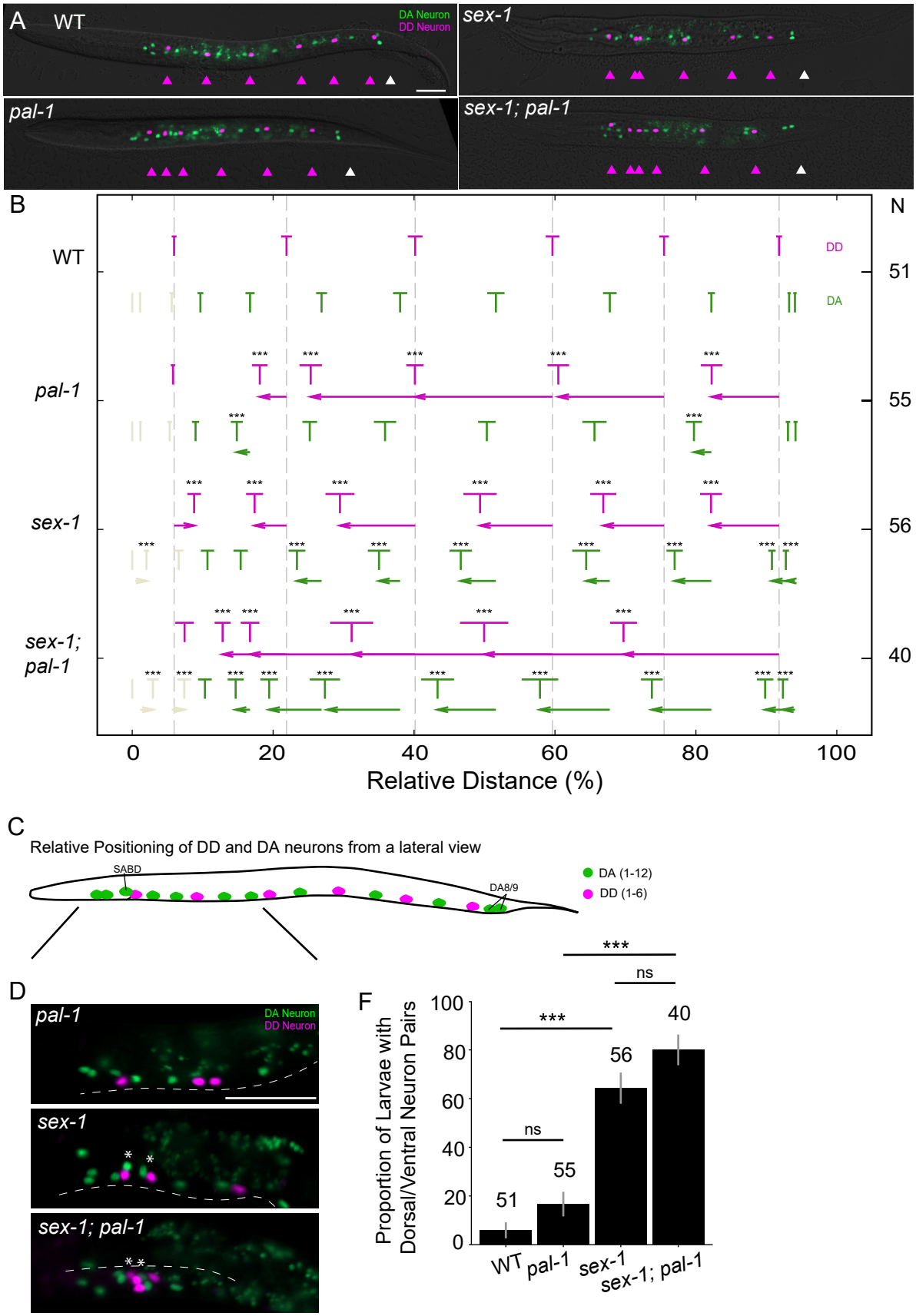
A
WT
DA Neuron
DD Neuron
sex-1
pal-1
sex-1; pal-1
B
N
WT
pal-1
sex-1
sex-1;
pal-1
DD
DA
51
55
56
40
0
20
40
60
80
100
Relative Distance (%)
C
Relative Positioning of DD and DA neurons from a lateral view
SABD
DA8/9
DA (1-12)
DD (1-6)
D
pal-1
DA Neuron
DD Neuron
sex-1
sex-1; pal-1
F
Proportion of Larvae with
Dorsal/Ventral Neuron Pairs
100
80
60
40
20
0
51
55
56
40
ns
***
ns
***
WT
pal-1
sex-1
sex-1; pal-1

FIG 4

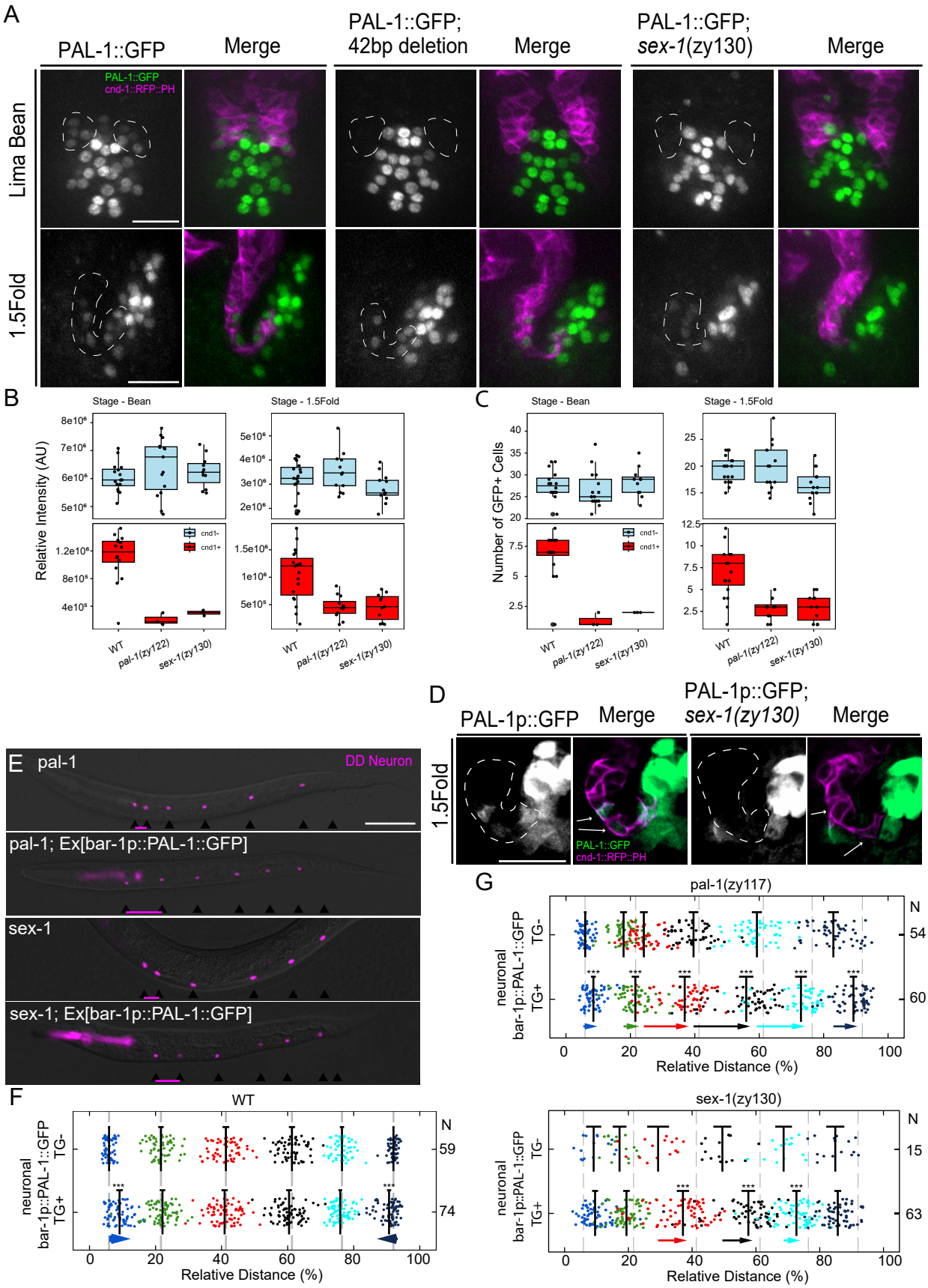
A
PAL-1::GFP
Merge
PAL-1::GFP; 42bp deletion
Merge
PAL-1::GFP; sex-1(zy130)
Merge
Lima Bean
1.5Fold
PAL-1::GFP
cnd-1::RFP::PH
B
Stage - Bean
Stage - 1.5Fold
Relative Intensity (AU)
cnd1-
cnd1+
WT
pal-1(zy122)
sex-1(zy130)
C
Stage - Bean
Stage - 1.5Fold
Number of GFP+ Cells
D
PAL-1p::GFP
Merge
PAL-1p::GFP; sex-1(zy130)
Merge
1.5Fold
E
pal-1
DD Neuron
pal-1; Ex[bar-1p::PAL-1::GFP]
sex-1
sex-1; Ex[bar-1p::PAL-1::GFP]
F
WT
neuronal bar-1p::PAL-1::GFP
TG-
TG+
N
59
74
Relative Distance (%)
G
pal-1(zy117)
54
60
sex-1(zy130)
15
63

FIG 5